Dimensionless Collisionality Scans for Core Particle Transport in JET

T. Tala[1], P. Mantica[4], A. Salmi[1], C. Bourdelle[3], C. Giroud[4], J. Hillesheim[4], C. Maggi[4], L. Meneses[5], M. Maslov[4], S. Menmuir[4], S. Moradi[6], S. Mordijck[7], V. Naulin[8], H. Nordman[9], J. Juul Rasmussen[8], G. Sips[10], A. Sirinelli[3], M. Tsalas[11], H. Weisen[12] and JET contributors

EUROfusion Consortium, JET, Culham Science Centre, Abingdon, OX14 3DB, UK
[1]VTT, P.O. Box 1000, FI-02044 VTT, Espoo, Finland
[2]Istituto di Fisica del Plasma, via Cozzi 53, 20125 Milano, Italy
[3]CEA, IRFM, F-13108 Saint-Paul-lez-Durance, France
[4]CCFE, Culham Science Centre, Abingdon, OX14 3DB, UK
[5]Instituto de Plasmas e Fusão Nuclear, IST, Universidade de Lisboa, Portugal, IST, Lisbon, Portugal
[6]Ecole Polytechnique, CNRS UMR7648, LPP, F-91128, Palaiseau, France
[7]College of William & Mary, Virginia, USA
[8]Danish Technical University Physics, Lyngby, Denmark
[9]Chalmers University of Technology, Göteborg 41296, Sweden
[10]European Commission, Brussels, Belgium
[11]DIFFER, Nieuwegein, Netherlands
[12]CRPP, Lausanne, Switzerland
*See the Appendix of F. Romanelli et al., Proc. of the 25th IAEA Fusion Energy Conference 2014, Saint Petersburg, Russia

1. Introduction

Particle transport and fuelling are major open questions in understanding the ITER physics basics [1]. Extensive database studies on density peaking on several tokamaks showed that in the H-mode plasmas, collisionality is the most important parameter determining the density peaking [2,3]. The neutral beam fuelling source was found to be the second most important factor. On the other hand in L-mode, the plasma internal inductance l_i was to found to be the key factor in determining the density peaking [4].

To verify the trends found in references [2-4], particle transport has been studied in JET by performing a dimensionless collisionality scan both in H-mode (ITER like wall) and L-mode (carbon wall) plasma. Gas puff modulation technique was exploited in all plasma discharges to obtain perturbative particle transport coefficients. Furthermore, density perturbation will shed light on the question from where this peaking is coming to understand details of the beam and neutral particle source. However, the analysis of the neutral particle source and the edge and SOL particle transport studies are reported in another paper in this conference [5].

2. Experimental Set-Up for Collisionality Scans and Gas Puff Modulation Technique

The H-mode discharges were run with the strike point in the corner (not located at vertical nor horizontal divertor tiles) so that the operational space to vary density was largest. The typical plasma parameters in this low triangularity baseline scenario plasmas were B_t=2.7T, I_p=2.0MA, n_{e0}=6x10^{19}m^{-3}, T_{e0}=3.5keV and Z_{eff}~1.3. The gas puff modulation was performed with a gas valve at the top of the machine at 3Hz frequency using rectangular waveform, the rate varying from 0 to 6x10^{22}s^{-1} at 30% duty cycle. Another gas injection module at the divertor location was used to keep the volume averaged density constant.

In order to test the linearity of the gas puff modulation technique, the modulated gas puff rate was doubled for one of the discharges. The phase profile stayed the same while the amplitude doubled, thus giving confidence that fuelling from the gas puff modulation at this level is linear and does not perturb the plasma background transport. Therefore, in determining the transport coefficients, the assumption that the background is time-independent seems valid.

The plasma response (electron density modulation) is measured with a multi-band profile reflectometer capable of good spatial and temporal resolution [6] and high resolution Thomson Scattering. This data was found to agree well with respect to steady-state profiles and the amplitude, but the there is a significant difference in the modulation phase profile between the reflectometer and Thomson scattering diagnostics. This is issue is being reviewed for the time being.

3. Results from the Collisionality Scans

3-point collisionality υ* scans were performed both in JET H-mode and L-mode plasmas. In each scan, roughly a factor of 5 in υ* was achieved by scanning I_p from 1.7MA to 2.5 MA and B_t from 2.0T to 3.0T, respectively. The dimensionless parameters, q, ρ^*, β_n and T_i/T_e were matched very well within the H-mode scan, the difference between the shots being only a few % (<10% in worst case). This is illustrated in figure 1. Even the temperature gradient length R/L_T was constant within the scan. The volume averaged density is very similar, within 5% between the three discharges, operationally keeping density constant when scanning the plasma current to such an extent is in general far from trivial in all metal device.

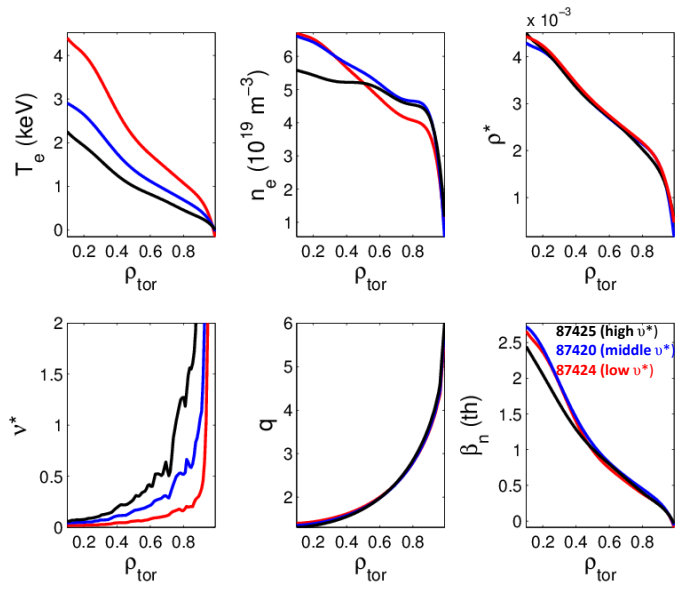

While the volume averaged n_e is very similar, the density profile shape is significantly more peaked at low υ*, as shown in figure 2 (left frame). The density peaking factor, defined here as R/Ln_e, increases in the inner core (r/a=0.3) from 0.3 to 2.7 and in the outer core (r/a=0.8) from 1.6 to 3.5 when the volume averaged υ* decreases from 0.47 to 0.09. Similar dimensionless 3-point υ* scan was executed with the carbon wall in L-mode by scanning υ* by a factor of 4. Unlike in H-mode, no change in R/Ln_e was observed, indicating same particle transport coefficients in each shot, shown in figure 2 (right frame).

Figure 1. The main parameters in the JET dimensionless 3-point H-mode collisioality scan.

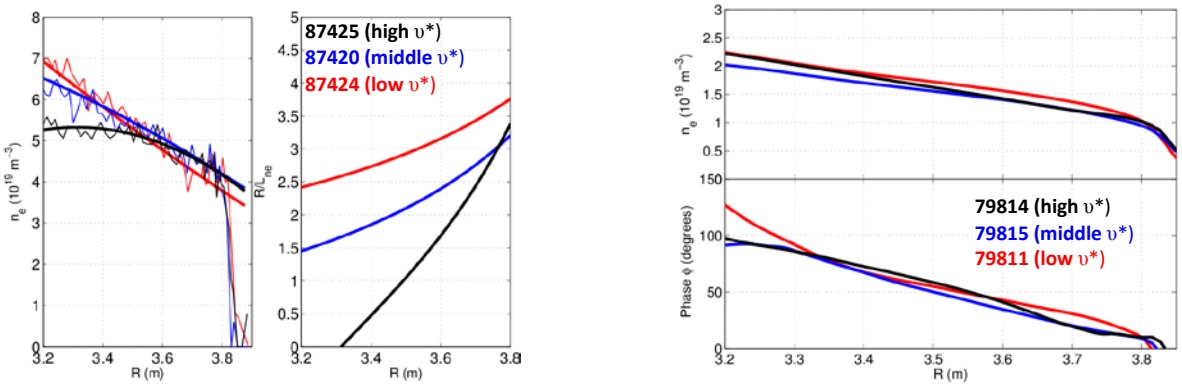

Figure 2. Left frame: Density and density peaking profiles for the same discharges as in figure 1. Right frame: Density profiles and the phase profiles of the density modulation for the dimensionless L-mode collisionality scan.

The results from both of the dedicated H-mode and L-mode scans are consistent with the earlier density database results in L-mode [4] and H-mode [2,3] with respect to collisionality dependence of density peaking. Opposed to JET, on DIII-D no υ* dependence on collisionality was reported either H (or L-mode) within the same range of the volume averaged υ* [7]. It is to be noted that the scan covered only a factor of 2 and besides NBI heating, additional ECH was used in accessing the low υ* point.

4. Particle Transport Coefficients and a Comparison to Theory

The key question is what the fraction of inward convection versus NBI particle source and neutral particle source is in contributing to the observed relatively strong density peaking. One can point out that the NBI fuelling rate increases from 0.8×10^{21} 1/s to 2.3×10^{21} 1/s within the collisionality scan. Therefore, one has to obtain the particle transport coefficients from the gas puff modulation data to distinguish the relative roles of fuelling versus transport. The experimental data from the gas puff modulation analysis indicates that a narrow neutral fuelling profile and peaked at the edge is most consistent with all transport analyses and thus does not contribute to density peaking even at ρ=0.8 [5]. SOLPS modelling is on-going for more precise neutral source calculation and edge particle transport analysis.

The transport coefficients have been determined using ASTRA transport code by choosing the diffusion D and convection v in such way that the least square error between the simulated and experimental steady-state n_e, and the modulation amplitudes $A(n_e)$ and phases $\Phi(n_e)$ is minimized. This technique is analogous to the analysis method of the JET NBI modulation experiment [8]. The beam particle source is calculated with PENCIL. The results are shown in figure 3 for JET pulse 87420 which is the intermediate shot in the collisionality scan. Steady-state and modulation amplitude $A(n_e)$ of n_e are well reproduced with the inferred D and v on the bottom right panel. Also the phase of n_e modulation $\Phi(n_e)$ is well reproduced, but only against HRTS data. No combination of D and v can reproduce the phase from the reflectometry. There is an issue identified with the analysis of the profile reflectometry data and this is being assessed right now. The same set of D and v reproduces also the second harmonic data and is thus an extra confidence on the accuracy of the analysis.

To quantify the relative level of density peaking originating from the fuelling sources versus inward pinch, the density peaking factor Rv/D by using the determined D and v are compared to the measured peaking R/L_{ne}. These D and v from Astra optimization include the NBI fuelling source term and therefore, they give the peaking factor due to only transport effects. This is shown in figure 4.

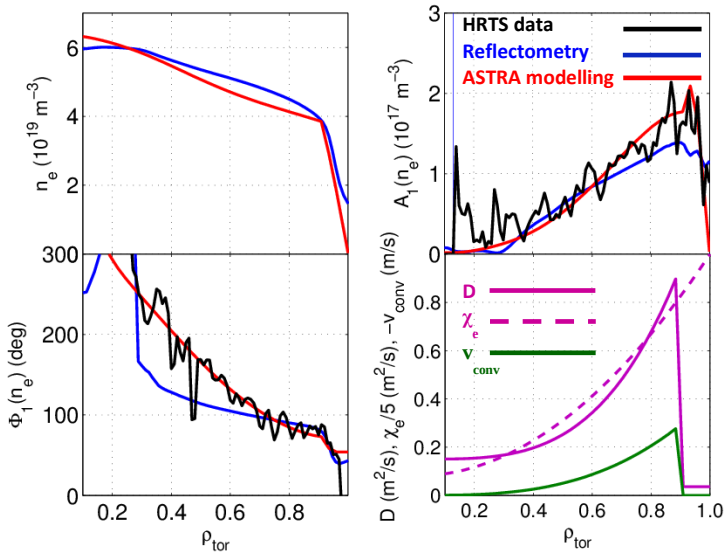

Figure 3. Determination of the particle transport coefficients for pulse no 87420.

Furthermore, the density peaking factor from linear gyro-kinetic with GYRO and fluid runs with the Weiland model were added for comparison. GYRO runs were linear, electro-magnetic, and with drift-kinetic electrons at k_y=0.3. The results turned out to be sensitive to the choice of k_y [9]. Weiland fluid runs were also at k_y=0.3. R/L_n was searched for the root of the interpolated normalized electron flux as a function of a/L_{ne} by assuming zero particle flux.

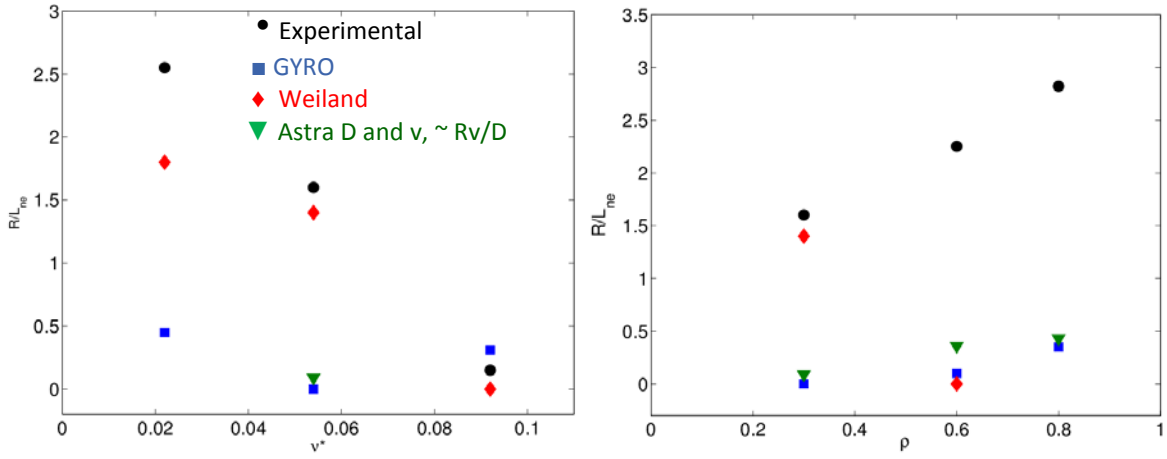

Figure 4. Left frame: Density peaking as a function of υ* from the 3-point υ* scan at ρ=0.3 and right frame: density peaking for JET pulse no 87420. Both frames include the experimental, Astra inferred and the modelled GYRO and Weiland density peaking profiles.

There are two very important messages in figure 4. Firstly, the difference between the measured experimental R/L_{ne} and the ones from Astra that include the NBI fuelling contribution show that the NBI fuelling seems to play a major role in contributing to the density peaking. In fact, for this JET, fuelling is the dominant factor as the part below the green triangles are due to inward pinch and the part above with respect to the experimental ones (black points) are due to NBI fuelling. Secondly, GYRO with the assumptions discussed above predicts very low density peaking, which is actually consistent with the density peaking factors from the transport modelling (green triangles).

5. Summary

Density peaking increases in the inner core (*r/a*=0.3) from 0.3 to 2.7 and in the outer core (*r/a*=0.8) from 1.6 to 3.5 when υ* decreases from 0.47 to 0.09 in JET H-mode plasmas while density peaking does not depend on υ* in JET L-mode plasma. For this particular scan, experimental evidence indicates that a dominant part of this peaking originates from NBI fuelling and inward pinch is a subdominant fraction. This is supported by the simple linear runs with GYRO although much more work is needed here to make a conclusion. More discharges are needed to quantify more precisely the fractions of these two contributions and also much more work is required on the modelling front to make exact comparisons.

Acknowledgement. This work has been carried out within the framework of the EUROfusion Consortium and has received funding from the Euratom research and training programme 2014-2018 under grant agreement No 633053. The views and opinions expressed herein do not necessarily reflect those of the European Commission.

[1] A. Loarte *et al*., Nucl. Fusion **53**, 083031 (2013).
[2] H. Weisen *et al*., Plasma Phys. Control. Fusion **48**, A457 (2006).
[3] C. Angioni *et al*., Nucl. Fusion **47** 1326–1335 (2007).
[4] H. Weisen *et al*., Plasma Phys. Control. Fusion **46**, 751 (2004).
[5] A. Salmi *et al.*, 42nd EPS Conference, Lisbon, Portugal, 22-26 June 2015.
[6] A. Sirinelli *et al*., Review of Scientific Instruments **81**, 10D939 (2010).
[7] E. Doyle *et al*., 24th IAEA Fusion Energy Conference, San Diego, USA, October 8-13, 2012.
[8] T. Tala *et al.* Phys. Rev. Lett. **102**, 075001 (2009).
[9] C. Bourdelle *et al.*, Phys. Plasmas **14,** 112501 (2007).